

Role of Advanced Magnetic Resonance Imaging (MRI) in the Evaluation of Renal Masses: A Prospective Cross-Sectional StudyNavneet Ranjan Lal¹, Deb K Boruah², Gaurav Raj³, Rajnikant R. Yadav⁴¹Senior Resident, Department of Radiology, Dr. Ram Manohar Lohia Institute of Medical Sciences, Lucknow, UP²Associate Professor, Department of Radiology, All India Institute of medical sciences, Guwahati, Assam³Professor and Head of Department, Department of Radiology, Dr. Ram Manohar Lohia Institute of Medical Sciences, Lucknow, UP⁴Associate Professor, Department of Radiology, Sanjay Gandhi Postgraduate Institute of Medical Sciences, Lucknow, UP

Received: 10-01-2024 / Revised: 13-02-2024 / Accepted: 10-03-2024

Corresponding Author: Dr. Navneet Ranjan Lal

Conflict of interest: Nil

Abstract:

Our study was an observational prospective study, which aims to evaluate the role of advanced MRI techniques in the characterization and differentiation of various renal masses. 37 patients were subjected to conventional, diffusion-weighted (DWI) and dynamic contrast-enhanced (DCE) MR imaging techniques and findings were correlated with the histopathological examination (HPE). Out of 37 patients, 27 were malignant (73%) renal masses had mean apparent diffusion coefficient (ADC) value of 1.14 ± 0.09 [SD] $\times 10^{-3}$ mm²/s and 10 were benign (27%) renal masses lesions had mean ADC value of 1.69 ± 0.63 [SD] $\times 10^{-3}$ mm²/s with a statistically significant difference (p-value 0.0001). There was a mean cut-off ADC value of 1.20×10^{-3} mm²/s in differentiating malignant from benign renal masses with a 90% of sensitivity and 82% of specificity. DCE-MRI showed higher relative contrast enhancement rates and indices in clear cell renal cell carcinoma (RCC) than non-clear cell RCCs.

Keywords: Diffusion, contrast-enhancement, renal tumor.

This is an Open Access article that uses a funding model which does not charge readers or their institutions for access and distributed under the terms of the Creative Commons Attribution License (<http://creativecommons.org/licenses/by/4.0>) and the Budapest Open Access Initiative (<http://www.budapestopenaccessinitiative.org/read>), which permit unrestricted use, distribution, and reproduction in any medium, provided original work is properly credited.

Introduction

Uses of more available cross-sectional imaging techniques increase the incidental detection of renal masses. [1] Previous studies showed higher rate of unnecessarily resection of benign renal masses. [2,3] Most of the renal incidentaloma shows malignancy followed by benignity in 20–25%. [2,3] It is important to characterize and differentiate these renal Incidentalomas because of treatment varies on the nature and grading of the lesion. [4,5]

With common use of MDCT and conventional MRI techniques characterization and differentiations of various renal masses difficult sometimes and which increases the number of nephrectomies performed on benign renal lesions from 16 to 33%.⁶ With the use of advanced MRI techniques like different b-value DWI, ADC mapping and DCE-MRI increases the MRI performance for characterization and differentiations various renal lesions. [5] The Brownian movement of water molecules in vivo can be assessed with diffusion and the degree of diffusion can be quantified by ADC value. [7] DCE-MRI used to characterize tumors, its nature,

cystic or necrotic changes within a tumor which facilitate the accurate tumor differentiating and a very close radiological diagnosis. [7] So advanced MRI techniques helps in selecting therapeutic options, treatment response and post-treatment outcomes. [8,9] DCE-MRI was also able to discriminate between the RCC subtypes. [6,10] In patients with compromised renal function, DWI can be helpful in the characterization of various renal masses. [11] Our study aims to evaluate the role of advanced MRI techniques in the characterization and differentiation of various renal masses.

Materials and Methods

A hospital-based prospective study was carried out in 37 patients of various renal masses.

The study was carried out from July 2018 to June 2019 in the department of Radio-diagnosis in a tertiary referral center. Institutional ethics review committee permission was obtained.

Inclusion Criteria:

- Patient with USG or CT scan detected solid appearing renal lesions.
- Indeterminate renal lesion on USG and or CT scan.
- Complex renal cyst.... Bosniak category (III & IV)
- Age 20-70 years

Exclusion Criteria:

- Simple renal cyst- Bosniak category (I & II)
- Post-traumatic renal hematoma
- Post-treated known patient of renal cell carcinoma.

MRI protocol: Conventional and advanced MRI techniques of the KUB region were done in all patients using a 1.5 Tesla Avanto B15 system MRI scanner by use of a 16 Channel Body Array Anterior coil. Table 1 showed the various parameters used during MRI scanning.

Conventional MRI sequence analysis: Morphological analysis of the renal masses were done on basis of T1-weighted, T2-Weighted and fat-suppressed T2-Weighted sequences and analyzed for

1. Appearance of renal mass on T1-weighted, T2-Weighted sequences.
2. Local tumor infiltration into the adjacent perinephric fats and para-renal space was assessed on T2-Weighted, fat-suppressed T2-Weighted, diffusion-weighted and dynamic post-gadolinium sequences.
3. Involvement of renal vein and IVC.
4. The largest dimension of renal mass was measured on T2-Weighted and post-gadolinium sequences.

Diffusion-weighted MR sequence: Different b-value diffusion-weighted sequences were obtained to analyze the diffusion characteristics of the renal masses. ADC values of renal masses were obtained in each set of ADC images of b-values 400, 800 and 1000 sec/mm² and finally mean ADC value was obtained.

Calculation of ADC value in renal masses: Same operating system console of Siemens syngo. via was used by two radiologists to calculate the ADC value of renal lesions by using ROI(region of interest) techniques. Equal sizes four ROIs were used to obtain the ADC values of renal lesion in their solid appearing component or enhancing septa or enhancing complex cyst wall.

Dynamic contrast-enhanced MRI (DCE-MRI) sequence: This MRI sequence is consisted with a pre-contrast and one each post-gadolinium corticomedullary and nephrographic phases. This

whole sequence needs 6-8 minutes. The post-gadolinium phases were obtained after intravenous injection of gadolinium (0.1 mmoles/kg body weight) after 40-45 seconds. About 40 sec intervals were kept between the post-gadolinium corticomedullary and nephrographic phases.

Semi-quantitative signal intensity measurement on DCE-MRI: The MRI signal intensity on pre-contrast T1-Weighted images, post-gadolinium corticomedullary and nephrographic images were obtained from the normal appearing renal parenchyma and renal masses by placing equal sizes ROIs and used for calculating relative contrast enhancement rate (CER) in both post-gadolinium corticomedullary and nephrographic images by using the formula, [CER=SI in corticomedullary phase or nephrographic phase - SI in precontrast/ SI in precontrast] 12 and relative contrast enhancement index (CEI) by using formula, [CEI= CER renal tumor/ CER normal appearing renal parenchyma].¹²

Biopsy: USG-guided core needle biopsies were performed in n=27 patients of renal space occupying masses. Four patients with renal abscesses were confirmed after catheter drainage of abscess drainage. Biopsy was not done in 3 patients with benign-appearing complex renal cysts (Bosniak category-III) and 3 patients with renal angiomyolipomas. The various conventional and advanced MRI sequences findings were compared with the histopathological examination.

Statistical analysis: All data analysis was performed by using SPSS, version 20. The ADC value of renal masses was compared with an independent t-test and one-way ANOVA. Receiver operating characteristic curve (ROC) analysis was done to obtain cut-off mean ADC values in various renal masses.

Results

Demography: Out of 37 patients with various renal masses, n=10 were of benign and n=27 were malignant lesions. Histological subtypes of malignant renal masses were clear cell RCC in 16 patients (43.2%) (Figure 1) and non-clear cell RCC in 11 patients (29.7%) (Figures 2 & 3). Out of non-clear RCC, 7 patients (18.9%) were of papillary RCC (Figure 3), 2 patients (5.4%) of chromophobe RCC (Figure 2) and another 2 patients (5.4 %) of transitional cell carcinoma (TCC) (Figure 4). The mean of the largest dimension of the benign renal masses was 5.83±2.6[SD] cm while 7.64±2.9[SD] cm for malignant renal masses. Of benign renal masses, 4 patients (10.8 %) were renal abscesses, n=3 (8.1%) Bosniak category II complex renal cyst and n=3 patients (8.1%) were angiomyolipoma.

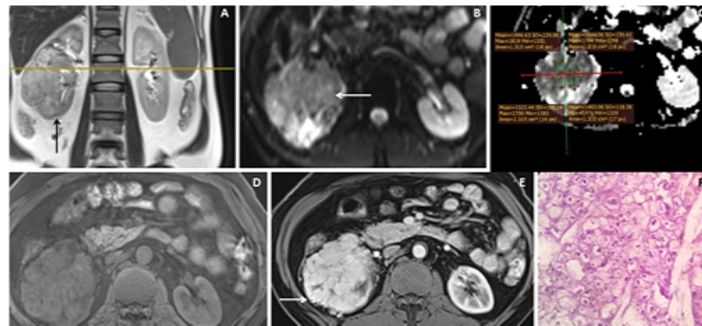


Figure 1: 60 years male with clear cell RCC

Coronal T1WI and T2FS images (A & B) shows a large T1 iso, T2 hypo to mixed- signal intensity lesion in the left kidney with T2 hypointense capsule (arrow).

Axial DWI and ADC map images (C & D) shows heterogenous patchy diffusion restriction with

variable ADC value (arrow). Axial post- contrast T1W fat-suppressed image (E) shows mild heterogeneous enhancement of the lesion with areas of necrosis. HPE image (F) with 40 X shows the Clear cell RCC.

373x182mm (96 x 96 DPI)

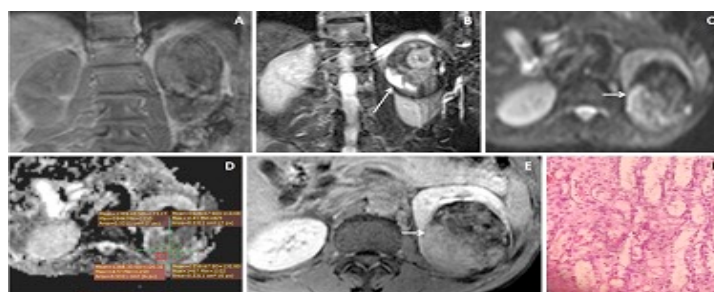


Figure 2: 51 year's male patient with Chromophobe RCC

Coronal T2WI (A) image shows a lobulated is to slight hyperintense lesion in the mid and lower polar regions of right kidney (arrow).

Axial DWI and ADC map images (C & D) shows strong solid diffusion restriction (arrow) with low

ADC value. ADC map image (C) also shows the way of ROI placement for ADC value calculation. HPE image (F) with 40 X shows the Chromophobe RCC.

324x167mm (96 x 96 DPI)

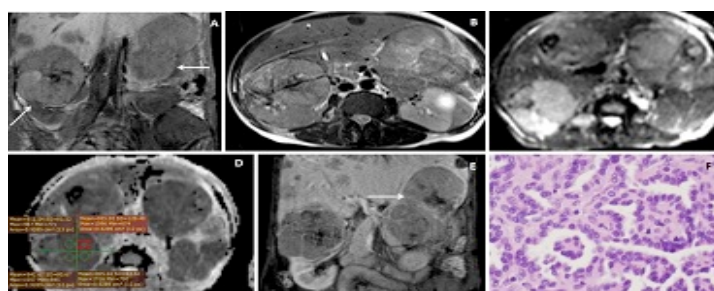


Figure 3: 70 years male patient with bilateral Papillary RCC

The coronal T1WI and axial fat-suppressed T2WI (A and B) images show T1 isointense and T2 iso to slight hypointense lesions in the both kidneys (arrows). DWI and ADC map (C & D) images show solid diffusion restriction with low ADC value. On fat-suppressed T1W post-contrast image (E) shows mild to moderate heterogeneous

enhancement with nonenhancing eccentric necrosis.

HPE image (F) with 40 X shows the Papillary RCC.

379x190mm (96 x 96 DPI)

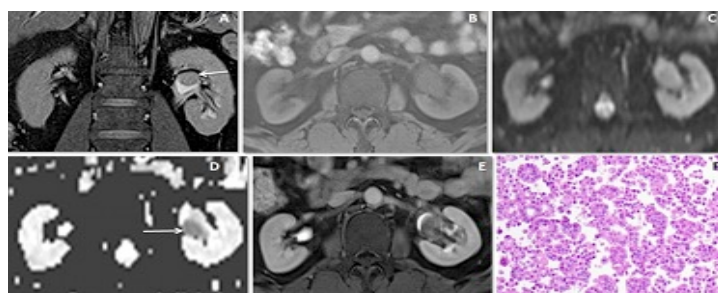


Figure 4: 45 year’s male patient with TCC

Fat-suppressed T2WI and axial fat-suppressed T1WI images (A and B) shows an ill-defined isointense lesion noted in the left renal pelvis (arrow). Axial DWI and ADC map (C and D) images shows patchy diffusion restriction with low ADC value (arrow). Axial fat-suppressed T1WI post-contrast image (E) shows subtle enhancement of the lesion. HPE image 40 x (F) shows the Transitional cell carcinoma (TCC).

307x167mm (96 x 96 DPI)

T1W and T2W signal intensity of renal lesions:

Most of the renal masses showed low to hypo intensity on T1WI in 16 patients (43.2%). T2WI heterogeneous mixed-signal intensities observed in 20 patients (54.1%) followed by T2WI high signal intensities in 15 patients (40.5%).

Diffusion-weighted imaging (DWI) findings:

Of 37 patients, 25 patients (67.6%) showed diffuse homogenous solid diffusion-restriction with low ADC value on DWI images followed by peripheral restriction in 5 patients (13.5%) and patchy diffusion-restrictions in 4 patients (10.8%). Cut-off mean ADC value of $< 1.20 \times 10^{-3} \text{ mm}^2/\text{s}$ was obtained after ROC curve analysis, which showed 24 renal masses (64.9%) as malignant and 13 (35.1%) as benign, shown in Table 2. Benign renal lesions showed mean ADC value of $1.69 \pm 0.63[\text{SD}] \times 10^{-3} \text{ mm}^2/\text{s}$ while malignant showed

$1.14 \pm 0.09[\text{SD}] \times 10^{-3} \text{ mm}^2/\text{s}$. statistically significant difference was found between the mean ADC value of benign and malignant renal lesions (p-value 0.0001). The mean ADC values of various renal lesions. Among the malignant renal masses, highest mean ADC was observed in Chromophobe RCC ($1.33 \pm 0.01 \times 10^{-3} \text{ mm}^2/\text{s}$) and lowest in Papillary RCC ($1.03 \pm 0.04 \times 10^{-3} \text{ mm}^2/\text{s}$). The mean ADC value of papillary RCC showed statistical significance with chromophobe RCC with p-value 0.01.

However, no statistical significance difference was found between the mean ADC value of clear cell RCC and papillary RCC (p-value 0.13).

ROC curve analysis reveals a cut-off mean ADC value of $1.20 \times 10^{-3} \text{ mm}^2/\text{s}$ for differentiating renal masses with various sensitivities and specificities shown in Table 3.

DCE-MRI findings: Out of 37 renal masses, on DCE-MRI, 30 renal masses (81.1%) showed malignant characteristics while 7 (18.9%) masses showed benign characteristics on basis of signal intensity (SI), CER and CEI.

The signal intensities of various renal masses shown in Table 4, CER values in Table 5 and CEI values in Table 6. Table 7 showed comparison between the diffusion-weighted and post gadolinium sequences for differentiating various renal masses.

Table 1 : Parameters used in various MRI sequences for KUB region for renal masses

MRI Sequences	Repetition time (TR)	Time of echo (TE)	Flip angle	Field of view (FOV)
T1WI (axial)	202ms	4.7ms	70°	262x350
T2WI (axial)	4000ms	103ms	150°	262x350
Turbo spine echo T2 WI with fat-suppression (Axial and coronal)	4000ms	103ms	150°	262x350
SS-EPI-DWI (b=400, 800, 1000s/mm ²)	3600ms	87ms	90°	262x350
T1WI fat-suppression dynamic contrast-enhanced MRI (DCE-MRI)	202ms	9.7ms	70°	262x350

Table 2 : Showing the mean ADC values of various renal masses in 37 patients

Renal lesion	Number of renal lesion(n)	Mean ADC value of lesion X 10 ⁻³ mm ² /s
Benign renal lesions	10	1.69 ± 0.63[SD]
Malignant renal lesions	27	1.14 ± 0.09[SD]
Complex Renal Cyst	3	2.56 ± 0.34[SD]
Clear cell RCC	16	1.15 ± 0.03[SD]

Papillary RCC	7	1.03±0.04 [SD]
Chromophobe RCC	2	1.33±0.01 [SD]
Renal angiomyolipoma	3	1.41±0.02 [SD]
Renal abscess	4	1.24±0.11 [SD]
Renal transitional cell carcinoma (TCC)	2	1.26±0.03 [SD]

Table 3 : ROC curve analysis at different 'b' values DWI images for characterization of various benign and malignant renal space occupying masses in 37 patients

Diffusion Gradient(s/mm ²)	Cut-off mean ADC (ADCx10 ⁻³ mm ² /s)	Sensitivity (%)	Specificity (%)
b-400	1.20	98	19
b-800	1.20	90	82
b-1000	1.20	71	93

Table 4: Mean Signal intensity (SI) values of the normal appearing renal parenchyma and renal masses on Precontrast, corticomedullary phase and nephrographic phase of DCEMRI in 37 patients

Parameters	Precontrast	Corticomedullary phase	p-value	Nephrographic phase	p-value
Normal appearing renal parenchyma	130±2.5	160.9±8.2		152.6±8.7	
Benign renal masses	126.8±2.1	148.9±16.6	0.0005	145.6±16.2	0.001
Malignant renal masses	132.2±5.8	172±8.3		161.7±10.5	
Clear cell carcinoma	133.1±7.4	176.1±8.4	0.0005	167.6±9.7	0.0005
Non-clear cell carcinoma	130.9±1.92	166.2±3.1		153.1±2.46	
Papillary carcinoma	130.1±2	165.6±3.8		153.1±3.2	
Chromophobe cell carcinoma	132±0.1	167±0.2		153±0.1	
Transitional cell carcinoma	132.5±0.71	167.5±0.71		153±0.1	
Angiomyolipoma	126±1.73	149.6±5.8		146.3±3.7	
Renal abscess	128±1.8	148.7±27.2		144.2±26.2	
Complex renal cyst	126±2.6	148.3±7.3		146.6±11.3	

Table 5: Relative contrast enhancement rate (CER) values of various renal masses on corticomedullary phase and nephrographic phase of DCE-MRI in 37 patients

Parameters	Corticomedullary phase	p-value	Nephrographic phase	p-value
Benign renal masses	0.17±0.13	0.001	0.18±0.15	0.017
Malignant renal masses	0.29±0.04		0.22±0.05	
Clear cell carcinoma	0.32±0.04	0.0005	0.25±0.04	0.033
Non-clear cell carcinoma	0.26±0.01		0.17±0.01	
Papillary carcinoma	0.26±0.02		0.17±0.02	
Chromophobe cell carcinoma	0.26±0.0		0.16±0.0	
Transitional cell carcinoma	0.26±0.0		0.15±0.007	
Angiomyolipoma	0.18±0.04		0.16±0.03	
Renal abscess	0.16±0.21		0.12±0.20	
Complex renal cyst	0.17±0.07		0.30±0.14	

Table 6: Relative contrast enhancement index (CEI) values of various renal masses on corticomedullary phase and nephrographic phase of DCE-MRI in 37 patients

Parameters	Corticomedullary phase	p-value	Nephrographic phase	p-value
Benign renal masses	0.170±0.53	0.005	0.93±0.78	0.024
Malignant renal masses	1.57±0.84		1.66±0.85	
Clear cell carcinoma	1.93±0.91	0.0005	2.09±0.85	0.0005
Non-clear cell carcinoma	1.04±0.27		1.03±0.26	
Papillary carcinoma	1.15±0.29		1.03±0.21	
Chromophobe cell carcinoma	0.86±0.00		0.84±0.0	
Transitional cell carcinoma	0.86±0.0		1.22±0.53	
Angiomyolipoma	0.74±0.33		0.76±0.26	
Renal abscess	0.72±0.87		1.06±1.31	
Complex renal cyst	0.63±0.16		0.93±0.15	

Table 7: shows the comparison between the DWI and DCE-MRI pattern for differentiating various benign and malignant renal space occupying masses in 37 patients

Lesion characteristics	DWI		DCE-MRI	
	Benign (MeanADC $\geq 1.20 \times 10^{-3}$)	Malignant ($< 1.20 \times 10^{-3}$)	Benign	Malignant
Number of Lesions	13	24	7	30
Percentage (%)	35.1	64.9	18.9	81.1

Discussion

The advanced MRI sequences like DWI and DCE-MRI provide added advantages in characterizing and differentiating various renal space occupying masses and even their subtypes.

Though DCE-MRI imaging was better than DWI imaging in the characterizing and differentiation of various renal masses [6,7,10,11], however combined used of different b-value DWI and DCE-MRI sequences provide more better information than single use of either diffusion-weighted and post-gadolinium sequences for characterization and differentiation of various renal masses and RCC subtypes [10,11]. Benign renal masses had a higher ADC value as compared with malignant renal masses.

However accurate differentiation of various RCC subtypes with MR imaging can be possible and helps in management and prognostication of such patients. The non-papillary RCCs have a poorer prognosis than papillary RCCs [10].

In our study, low ADC value were encountered in malignant renal masses as comparable with the previously published studies [13,14]. The lowest ADC value was observed in Papillary RCC in our series, which as almost similar to the previous studies [15,16] shown in Table 8.

A statistical significant difference (p-value 0.01) was obtained between the mean ADC value of papillary RCC and Chromophobe RCC which also observed in previous study by Inci et al. [15].

Four out of 27 pathologically proven malignant cases had higher ADC value than the cutoff level (false negative) and 1 out of 10 benign cases had ADC values lower than $1.20 \times 10^{-3} \text{ mm}^2/\text{s}$ (false positive) and were misdiagnosed on basis of DWI and DCE-MRI, such similar observation was made by Taouli et al [17].

In the present study it was seen that 24 (64.9%) lesions out of 37 lesions showed malignant characteristics on DWI based on cut-off mean ADC value and 30 (81.1%) lesions showed malignant characteristics based on DCE-MRI pattern. Similarly 13 lesions showed benign characteristics on DWI and 7 lesions showed benign characteristics on DCE-MRI pattern.

So it was observed that DCE study is more accurate in differentiating benign and malignant lesion than DWI individually. Combination of advanced MRI

sequences like DWI and DCE-MRI provides better results as observed by the Taouli et al. [17]

Post-gadolinium enhancement pattern of various renal masses on basis of Precontrast and post-contrast signal intensity (SI) measurement in various phases of DCE-MRI added advantages in differentiation of various renal masses.

Study by Campbel et al. [18] showed greater degree of enhancement of clear cell RCC in corticomedullary phase with rapid contrast wash-out in reopgraphic phase as compared with the normal appearing renal parenchyma. [18] While papillary RCC showed less enhancement in the both corticomedullary and reopgraphic phases. Chandarana et al. [19] found 90.9 % sensitivity and 84.2% specificity on CER in the post-gadolinium corticomedullary phase for differentiating clear cell RCC from papillary RCC. In our study, there was a statistical significant difference of CER and CEI in differentiating clear cell RCC from non-clear cell RCC in the both post gadolinium phases. Study by Sun et al. [12] found the CEI values in corticomedullary phase are most effective to differentiate clear cell RCC from papillary RCC.

Limitations of the study: Relatively small sample size, the results can be vary to larger study sample, hence need future larger sample size study.

Conclusion

A close diagnosis of the various renal masses is essential for planning the proper treatment and avoiding unnecessary nephrectomy with the use of additional advanced MRI sequences like different b-value diffusion-weighted and dynamic post-gadolinium MR sequences. The values of signal intensity (SI), CER and CEI in the post-gadolinium images helpful in characterizing and differentiating various renal masses and even differentiating between the clear cell RCC from the nonclear cell RCC.

References

1. Krishna S, Leckie A, Kielar A, et al. Imaging of Renal Cancer. *Seminars in Ultrasound, CT and MRI*. 2020, 41[2];152-169.
2. Schieda N, Krishna S, Pedrosa I, et al. Active Surveillance of Renal Masses: The Role of Radiology. *Radiology* 2021.
3. Musaddaq B, Musaddaq T, Gupta A, et al. Renal Cell Carcinoma: The Evolving Role of

- Imaging in the 21st Century. *Seminars in Ultrasound, CT and MRI*; 2020,41[4];344-350.
4. Millet I, Doyon FC, Hoa D, et al. Characterization of small solid renal lesions: Can benign and malignant tumors be differentiated with CT? *IntBraz J Urol*. 2011;37(6):789–90.
 5. Aggarwal A, Das CJ, Sharma S. Recent advances in imaging techniques of renal masses. *World J Radiol*. 2022; 14(6): 137–150.
 6. Kim JH, Sun HY, Hwang J, et al. Diagnostic accuracy of contrast-enhanced computed tomography and contrast-enhanced magnetic resonance imaging of small renal masses in real practice: sensitivity and specificity according to subjective radiologic interpretation. *World J SurgOncol*. 2016; 14: 260.
 7. Messina C, Bignone R, Bruno A, et al. Diffusion-Weighted Imaging in Oncology: An Update. *Cancers* 2020, 12(6), 1493.
 8. Mahajan A, Deshpande SS, Thakur MH. Diffusion magnetic resonance imaging: A molecular imaging tool caught between hope, hype and the real world of “personalized oncology” *World J Radiol*. 2017; 9(6): 253–268. 2.
 9. Perrot TD, Zoua CS, Glessgen CG, et al. Diffusion-Weighted MRI in the Genitourinary System *J Clin Med*. 2022; 11(7): 1921.
 10. Wang H, Su Z, Xu X, et al. Dynamic Contrast-enhanced MRI in Renal Tumors: Common Subtype Differentiation using Pharmacokinetics. *Sci Rep*. 2017; 7: 3117.
 11. Goyal A, Sharma R, Bhalla AS, et al. Comparison of MDCT, MRI and MRI with diffusion-weighted imaging in evaluation of focal renal lesions: The defender, challenger, and winner! *Indian J Radiol Imaging*. 2018; 28(1): 27–36.
 12. Sun MR, Ngo L, Genega EM, et al. Renal cell carcinoma: dynamic contrast-enhanced MR imaging for differentiation of tumor subtypes—correlation with pathologic findings. *Radiology*. 2009;250(3):793-802.
 13. Goyal A, Sharma R, Bhalla AS, et al. Diffusion-weighted MRI in renal cell carcinoma: A surrogate marker for predicting nuclear grade and histological subtype. *Acta Radiol*. 2012;1;53(3):349–58.
 14. Sandrasegaran K, Sundaram CP, Ramaswamy R, et al. Usefulness of Diffusion-Weighted Imaging in the Evaluation of Renal Masses. *Am J Roentgenol*. 2010; 194(2):438–45.
 15. Inci E, Hocaoglu E, Aydin S, et al. Diffusion-weighted magnetic resonance imaging in evaluation of primary solid and cystic renal masses using the Bosniak classification. *Eur J Radiol*. 2012;81(5):815–20.
 16. Zhang HM, Wu YH, Gan Q, et al. Diagnostic Utility of Diffusion-weighted Magnetic Resonance Imaging in Differentiating Small Solid Renal Tumors (≤ 4 cm) at 3.0T Magnetic Resonance Imaging. *Chin Med J (Engl)* 2015; 128(11): 1444–1449.
 17. Taouli B, Thakur RK, Mannelli L, et al. Renal Lesions: Characterization with Diffusion weighted Imaging versus Contrast-enhanced MR Imaging. *Radiology*. 2009; 251(2):398–407.
 18. Campbell N, Rosenkrantz AB, Pedrosa I. MRI phenotype in renal cancer: is it clinically relevant? *Top MagnReson Imaging*. 2014;23(2):95-115.
 19. Chandarana H, Rosenkrantz AB, Mussi TC, et al. Histogram analysis of whole-lesion enhancement in differentiating clear cell from papillary subtype of renal cell cancer. *Radiology*. 2012;265(3):790-8.